European Journal of Pharmacology 917 (2022) 174750

Contents lists available at ScienceDirect

European Journal of Pharmacology

journal homepage: www.elsevier.com/locate/ejphar

Dichloroacetate reactivates pyruvate-supported peroxide removal by liver mitochondria and prevents NAFLD aggravation in NAD(P)$^+$ transhydrogenase-null mice consuming a high-fat diet

Claudia D.C. Navarro [a,**], Annelise Francisco [a], Tiago R. Figueira [a,b], Juliana A. Ronchi [a], Helena C.F. Oliveira [c], Anibal E. Vercesi [a], Roger F. Castilho [a,*]

[a] Department of Pathology, Faculty of Medical Sciences, University of Campinas (UNICAMP), Campinas, SP, 13083-888, Brazil
[b] School of Physical Education and Sport of Ribeirão Preto, University of São Paulo (USP), Ribeirão Preto, SP, 14040-907, Brazil
[c] Department of Structural and Functional Biology, Institute of Biology, University of Campinas (UNICAMP), Campinas, SP, 13083-862, Brazil

ARTICLE INFO

Chemical compounds studied in this article:
Sodium dichloroacetate (PubChem CID: 517326)

Keywords:
Liver steatosis
Non-alcoholic steatohepatitis (NASH)
Pyruvate dehydrogenase kinase (PDK)
Nnt mutation
C57BL/6J mouse

ABSTRACT

The mechanisms by which a high-fat diet (HFD) promotes non-alcoholic fatty liver disease (NAFLD) appear to involve liver mitochondrial dysfunction and redox imbalance. The functional loss of the enzyme NAD(P)$^+$ transhydrogenase, a main source of mitochondrial NADPH, results in impaired mitochondrial peroxide removal, pyruvate dehydrogenase inhibition by phosphorylation, and progression of NAFLD in HFD-fed mice. The present study aimed to investigate whether pharmacological reactivation of pyruvate dehydrogenase by dichloroacetate attenuates the mitochondrial redox dysfunction and the development of NAFLD in NAD(P)$^+$ transhydrogenase-null (*Nnt*$^{-/-}$) mice fed an HFD (60% of total calories from fat). For this purpose, *Nnt*$^{-/-}$ mice and their congenic controls (*Nnt*$^{+/+}$) were fed chow or an HFD for 20 weeks and received sodium dichloroacetate or NaCl in the final 12 weeks via drinking water. The results showed that HFD reduced the ability of isolated liver mitochondria from *Nnt*$^{-/-}$ mice to remove peroxide, which was prevented by the dichloroacetate treatment. HFD-fed mice of both *Nnt* genotypes exhibited increased body and liver mass, as well as a higher content of hepatic triglycerides, but dichloroacetate treatment attenuated these abnormalities only in *Nnt*$^{-/-}$ mice. Notably, dichloroacetate treatment decreased liver pyruvate dehydrogenase phosphorylation levels and prevented the aggravation of NAFLD in HFD-fed *Nnt*$^{-/-}$ mice. Conversely, dichloroacetate treatment elicited moderate hepatocyte ballooning in chow-fed mice, suggesting potentially toxic effects. We conclude that the protection against HFD-induced NAFLD by dichloroacetate is associated with its role in reactivating pyruvate dehydrogenase and reestablishing the pyruvate-supported liver mitochondrial capacity to handle peroxide in *Nnt*$^{-/-}$ mice.

1. Introduction

Non-alcoholic fatty liver disease (NAFLD) is among the myriad of metabolic disturbances that occur in response to high-fat diets (HFDs) (Buettner et al., 2007) and obesity (Chalasani et al., 2012). The ectopic accumulation of triglycerides in the liver is the hallmark of NAFLD; however, impaired insulin signaling and derangements in glucose, fructose, fatty acids, and ketone bodies metabolism are critical alterations that commonly accompany this disease (Alves et al., 2011; Go et al., 2016; Muriel et al., 2021). Studies in rodent models have revealed that HFD-induced NAFLD is associated with inhibitory serine phosphorylation of pyruvate dehydrogenase (PDH) in the liver (Alves et al., 2011; Go et al., 2016; Hwang et al., 2009; Saed et al., 2021; Schummer et al., 2008). Phosphorylation of PDH is a covalent inhibitory modulation of PDH and results in decreased mitochondrial pyruvate oxidation into acetyl-CoA (Rardin et al., 2009). The mechanisms of such inhibition seem to involve increased expression of pyruvate dehydrogenase kinase (PDK) isozymes in response to dietary lipid overload (Go et al., 2016; Hwang et al., 2009; Mapes and Harris, 1975; Schummer et al., 2008). In HFD-fed mice, molecular ablation of PDK2 or PDK4 resulted in attenuation of fatty liver and other metabolic alterations (Go et al., 2016;

* Corresponding author. Department of Pathology, Faculty of Medical Sciences, University of Campinas (UNICAMP), Rua Vital Brasil, 80, Campinas, SP, 13083-888, Brazil.
** Corresponding author. Department of Pathology, Faculty of Medical Sciences, University of Campinas (UNICAMP), Rua Vital Brasil, 80, Campinas, SP, 13083-888, Brazil.
E-mail addresses: claudia.doutunicamp@gmail.com (C.D.C. Navarro), rogerc@unicamp.br (R.F. Castilho).

https://doi.org/10.1016/j.ejphar.2022.174750
Received 1 November 2021; Received in revised form 14 December 2021; Accepted 5 January 2022
Available online 12 January 2022

Abbreviations

DCA	sodium dichloroacetate
GTT	glucose tolerance test
HFD	high-fat diet
IDH2	mitochondrial NADP-dependent isocitrate dehydrogenase
NAFLD	non-alcoholic fatty liver disease
NASH	non-alcoholic steatohepatitis
NNT	$NAD(P)^+$ transhydrogenase
Nnt	nicotinamide nucleotide transhydrogenase (gene)
PDH	pyruvate dehydrogenase
PDHE1α	E1α subunit of PDH
pPDHE1α (S293)	PDHE1α phosphorylated at serine 293
PDK	pyruvate dehydrogenase kinase
t-BOOH	tert-butyl hydroperoxide.

Hwang et al., 2009; Wu et al., 2018). Similar beneficial effects were observed in HFD-fed mice treated with the liver-specific pan-PDK inhibitor PS10 (Wu et al., 2018). Hence, PDKs became potential therapeutic targets for HFD-induced NAFLD and metabolic comorbidities such as glucose intolerance (Go et al., 2016).

Most molecular studies linking HFD to disturbances in pyruvate metabolism and NAFLD have been carried out in mice models bearing alleles with the spontaneous mutation in the nicotinamide nucleotide transhydrogenase (*Nnt)* from the C57BL/6J strain ($Nnt^{C57BL/6J}$) (Go et al., 2016; Hwang et al., 2009; Tso et al., 2014; Wu et al., 2018), which results in the absence of both $NAD(P)^+$ transhydrogenase (NNT) activity and mature protein expression in tissues from these mice. NNT is a main source of NADPH in liver mitochondria (Mailloux, 2018; Ronchi et al., 2016), which is required for several reductive processes, including peroxide removal (Agledal et al., 2010; Francisco et al., 2021). Mice devoid of functional NNT ($Nnt^{-/-}$) are particularly prone to HFD-induced NAFLD and redox abnormalities (Fisher-Wellman et al., 2016; Francisco et al., 2018; Navarro et al., 2017; Vercesi et al., 2018). We recently demonstrated that the inhibitory phosphorylation of PDH in HFD-fed $Nnt^{-/-}$ mice was associated with a slower removal of peroxide by isolated liver mitochondria, compared with *Nnt* wild-type mice ($Nnt^{+/+}$) maintained on an HFD when pyruvate was the carbon source for Krebs cycle (Navarro et al., 2017). Interestingly, the in vitro co-incubation of $Nnt^{-/-}$ liver mitochondria with sodium dichloroacetate (DCA), a pan-PDK inhibitor, promptly restored the peroxide removal ability to the levels of the genotype-matched chow-fed group (Navarro et al., 2017).

Because redox imbalance has been implicated in the pathophysiology of NAFLD (Mantena et al., 2008; Navarro et al., 2017; Spahis et al., 2016; Vercesi et al., 2018), impairment of mitochondrial peroxide metabolism due to PDH inhibition could play a role in the aggravation of HFD-induced NAFLD in mice lacking functional NNT. With that in mind, we investigated whether the DCA-driven PDH reactivation in HFD-fed $Nnt^{-/-}$ mice prevents the development of NASH and redox imbalance. The influence of the *Nnt* genotype on the effects of DCA was also assessed.

2. Material and methods

2.1. Reagents

ADP (catalog number A2754), glucose (#16301), 4-(2-hydroxyethyl)-1-piperazineethanesulfonic acid (HEPES; #H3375), L-malic acid (#M6413), oligomycin (#O4876), protease inhibitor cocktail (#P8340), pyruvic acid sodium salt (#P4552), DCA (#347795), *tert*-butyl hydroperoxide (t-BOOH, #458139), Trizma base (#T1503), Tween 20 (#P1379) and most other chemicals were obtained from Merck (St. Louis, USA). The mouse polyclonal antibody to PDHE1α (#110330, lot GR200453-8) and rabbit polyclonal antibody to E1α subunit of PDH (PDHE1α) phosphorylated at serine 293 (pPDHE1α (S293); #177461, lot GR196570-1) were purchased from Abcam (Cambridge, MA, USA). The HRP-conjugated secondary antibodies were rabbit anti-mouse (#554002) from BD Biosciences (San Diego, USA) and goat anti-rabbit (#7074) from Cell Signaling (Beverly, USA). Stock solutions of mitochondrial respiratory substrates were prepared in 20 mM HEPES buffer with the pH adjusted to 7.2 using KOH.

2.2. Animals and in vivo treatments

Congenic mice homozygously bearing the wild-type *Nnt* allele (C57BL/6JUnib $Nnt^{+/+}$) or the $Nnt^{C57BL/6J}$ mutated allele (C57BL/6JUnib $Nnt^{-/-}$) were provided by the Multidisciplinary Center for Biological Research in Laboratory Animals (CEMIB/Unicamp, Campinas, Brazil). One-month-old male mice of both genotypes were assigned by block randomization to two groups fed either a standard diet (chow, 3.9 kcal/g, 5% fat, 12% of total calories from fat) from Nuvital (Nuvilab CR1, Nuvital, Colombo, PR, Brazil) or an HFD (5.3 kcal/g, ~60% of total calories from fat) from PragSoluções (Hyperlipidic diet, PragSoluções Biociências, Jaú, SP, Brazil). Mice were maintained under standard laboratory conditions (22–24 °C, 12 h/12 h light/dark cycle) and fed on a standard chow diet or HFD for 20 weeks. In the last 12 weeks of treatment, groups were subdivided to receive DCA (1 g/L, ~80 mg/kg/day, based on a 40-g mouse) or NaCl (0.387 g/L) in their drinking water. Concentration, dose, and route of DCA administration were based on previous studies on murine models (Andreassen et al., 2001; Bian et al., 2009; Lingohr et al., 2001). The final samples sizes of each experimental group were: $Nnt^{+/+}$ Chow - DCA = 6; $Nnt^{+/+}$ Chow + DCA = 6; $Nnt^{+/+}$ HFD - DCA = 8; $Nnt^{+/+}$ HFD + DCA = 7; $Nnt^{-/-}$ Chow - DCA = 7; $Nnt^{-/-}$ Chow + DCA = 4; $Nnt^{-/-}$ HFD - DCA = 8; $Nnt^{-/-}$ HFD + DCA = 8. Fluid and food consumption were monitored, and animals were weighed weekly for the study duration. At the end of treatments, mice were subjected to a glucose tolerance test (GTT) and euthanized by cervical dislocation for liver removal. Livers were then processed for both histological evaluation and mitochondrial isolation.

The local Committee for Ethics in Animal Research approved the use of mice and experimental protocols (CEUA-UNICAMP, protocol number 5506-1/2020). The animal procedures complied with national Brazilian guideline number 13 for "Control in Animal Experiments," published on September 13th, 2013 (code 00012013092600005, available at <http://portal.in.gov.br/verificacao-autenticidade>).

2.3. Glucose tolerance test (GTT)

After 12 h of fasting, mice received 1.5 g/kg body weight of glucose solution by oral gavage. Blood samples were taken from the tip of the tail to determine blood glucose before (0 min) and after the glucose administration (15, 30, 60, 90, and 120 min). The glucose response to GTT was compared among groups considering each time of the curve.

2.4. Liver histology

Approximately 3-mm fragments of the two largest liver lobules were cut and processed for hematoxylin plus eosin staining as previously described (Navarro et al., 2017). Stained sections were blinded-evaluated under an optical microscope (Nikon Eclipse 80i). NAFLD was scored according to the NAFLD activity score (Kleiner et al., 2005), where scores ranging from 0 to 3 were assigned to ballooning (a grade of 3 was assigned when associated with Mallory's hyaline), microvesicular and macrovesicular steatosis, acinar inflammation and portal inflammation. The sum of these grades provides an overall NAFLD activity score (Kleiner et al., 2005).

2.5. Triglyceride content

The triglyceride content in the liver was measured by a commercial enzymatic-colorimetric kit (Roche-Hitachi Germany) as described previously (Navarro et al., 2017).

2.6. Mitochondrial isolation and redox state of mitochondrial nicotinamide nucleotides (NAD(P))

Mitochondria were isolated by homogenization of liver tissue followed by differential centrifugation of the homogenate, as previously described (Navarro et al., 2017). The redox state of mitochondrial NAD(P) was monitored in a spectrofluorometer (Hitachi F-4500, Tokyo, Japan) using excitation and emission wavelengths of 366 and 450 nm, respectively. Mitochondria were suspended at 0.5 mg/mL in 2 mL of reaction medium (125 mM sucrose, 65 mM KCl, 2 mM KH_2PO_4, 1 mM $MgCl_2$, 300 μM EGTA, and 10 mM HEPES buffer, pH 7.2) supplemented with malate (2.5 mM) plus pyruvate (5 mM) as respiratory substrates. The mitochondrial peroxide-metabolizing system supported by NADPH was challenged with exogenous *tert*-butyl hydroperoxide (t-BOOH, 15 μM). This organic peroxide is exclusively metabolized via glutathione reductase/glutathione peroxidase and thioredoxin reductase/peroxiredoxin systems at the expense of NADPH (Ronchi et al., 2016).

2.7. PDH expression and phosphorylation state

Isolated mitochondria were suspended in a medium containing phosphatase and protease inhibitors (150 mM NaCl, 1 mM EGTA, 1 mM Na_3VO_4, 1 mM NaF, 1% Tween 20, 1% protease inhibitor cocktail, and 50 mM Tris, pH 7.4) and diluted in standard Laemmli buffer (1:1). Western blot and immunodetection were performed according to Navarro et al. (2017). Briefly, the samples were electrophoresed (50 μg of protein per lane) using 8% SDS-PAGE. The resolved proteins were transferred to nitrocellulose membrane (0.45 μm, Bio-Rad, Hercules, CA) for 90 min at 120 V. The membranes were first reversibly stained by Ponceau and photographed as a protein loading control. After removing the Ponceau staining, the membranes were blocked with 5% dried milk. Immunodetection was carried out using polyclonal antibodies against PDHE1α (1:1000) or pPDHE1α (S293) (1:1000) and corresponding secondary antibodies (1:10000). Detection was performed using an enhanced chemiluminescence reagent (SuperSignal West Pico, Thermo Fisher, Waltham, MA, USA), and the luminescence signals were determined in a digital instrument (UVITEC, Cambridge, UK).

2.8. Statistical analyses

The results are representative traces, individual values, and mean ± standard deviation. The quantitative data were analyzed using Prism 6 software (GraphPad Software Inc.). Two-way ANOVA followed by Bonferroni as a post-hoc test was used to test differences between groups for most data, except for non-parametric data were evaluated using the Mann-Whitney test. The minimum significance level was set at $p \leq 0.05$.

3. Results

3.1. Mass of food intake and volume of fluid consumption in mice were affected by diet, but not by Nnt genotype or DCA treatment

The mass of food intake and volume of fluid consumption were evaluated weekly in the different experimental groups of $Nnt^{+/+}$ (Supplementary Table S1) and $Nnt^{-/-}$ (Supplementary Table S2) mice. No difference in fluid consumption and mass of food intake were observed over 12 weeks in mice receiving or not DCA in either chow or HFD. Additionally, HFD was a factor that significantly decreased food intake and fluid consumption in $Nnt^{+/+}$ ($p < 0.0001$ and $p < 0.01$, respectively) and $Nnt^{-/-}$ mice ($p < 0.0001$ and $p < 0.001$, respectively).

3.2. In vivo treatment with DCA fully recovers the ability of liver mitochondria from HFD-fed $Nnt^{-/-}$ mice to metabolize peroxide

Fig. 1A shows typical traces of the redox state of NAD(P) monitored in a spectrofluorometer during the metabolism of t-BOOH by isolated liver mitochondria from different experimental groups. Only the NAD(P) in the reduced state emits an endogenous fluorescence signal. During the metabolism of t-BOOH, glutathione reductase/glutathione peroxidase and thioredoxin reductase/peroxiredoxin detoxification systems oxidize NADPH, causing a drop in fluorescence. After all added t-BOOH is metabolized, fluorescence returns to basal levels because the reduced state of NAD(P) is restored (Ronchi et al., 2013). Isolated liver mitochondria from chow or HFD-fed $Nnt^{+/+}$ mice respiring on pyruvate plus malate show transient oxidation of matrix NAD(P)H after a bolus addition of the organic peroxide t-BOOH (Fig. 1A, left quadrants). No difference was observed in peroxide metabolism due to diet or DCA treatment in mitochondria from $Nnt^{+/+}$ mice (Fig. 1B).

As previously demonstrated (Ronchi et al., 2016), liver mitochondria from $Nnt^{-/-}$ mice metabolize peroxide slowly than those from $Nnt^{+/+}$ mice, even under a standard chow diet (Fig. 1A, upper quadrants). In $Nnt^{-/-}$ mice, the flux of pyruvate-derived carbons through NADPH-dependent isocitrate dehydrogenase (IDH2) is the main source of NADPH required for mitochondrial t-BOOH metabolism via the glutathione- and thioredoxin-dependent systems (Ronchi et al., 2016). This implies that PDH regulation could impact mitochondrial peroxide metabolism in $Nnt^{-/-}$ mice, which we previously demonstrated to occur when these mice are fed an HFD (Navarro et al., 2017). The results in Fig. 1A (right quadrants) and 1C show that isolated liver mitochondria from HFD-fed $Nnt^{-/-}$ have a compromised ability to metabolize t-BOOH. Indeed, the time required to recover the reduced state of NAD(P) after adding t-BOOH to mitochondria from HFD-fed $Nnt^{-/-}$ mice was two-fold longer when compared to the chow diet-fed group. Notably, in vivo treatment with the PDH activator DCA recovered the ability of HFD-fed $Nnt^{-/-}$ mice mitochondria to metabolize t-BOOH.

3.3. DCA treatment reduces body mass gain and improves glucose tolerance in HFD-fed $Nnt^{-/-}$ mice

The results in Fig. 2A and B shows that 20 weeks of HFD led to a higher body mass in $Nnt^{+/+}$ (44.7 ± 2.5 g) and $Nnt^{-/-}$ (43.4 ± 4.9 g) mice when compared with the respective control mice on chow diet (31.3 ± 2.6 g and 29.2 ± 1.5 g). Under DCA treatment, the $Nnt^{-/-}$ mice from the HFD group showed a significantly lower body mass gain (38.6 ± 5.6 g, $p = 0.008$). The DCA treatment did not affect the mass gain of mice fed on a chow diet or $Nnt^{+/+}$ mice on an HFD.

Oral GTT assessed glucose tolerance. No significant difference in glucose response was observed in $Nnt^{+/+}$ mice regardless of diet or DCA treatment (Fig. 2C). On the other hand, HFD-fed $Nnt^{-/-}$ mice showed higher resting and greater excursions of blood glucose levels when compared to the chow diet (Fig. 2D). Point-by-point comparison of GTT curves revealed that at 120 min the DCA treatment significantly decreased glycemia in HFD-fed $Nnt^{-/-}$ mice (165.9 ± 16.4 mg/dL vs. 208.0 ± 40.4 mg/dL, $p = 0.01$).

3.4. DCA prevents aggravation of NAFLD and reduces the mass and content of hepatic triglycerides in HFD-fed $Nnt^{-/-}$ mice

Figs. 3 and 4 respectively show representative microphotographs of livers sections and hepatic abnormalities scores from experimental groups of $Nnt^{+/+}$ mice. Under HFD, the liver of $Nnt^{+/+}$ mice presented increased mass and triglyceride content (Tables 1 and 2, respectively) accompanied by morphological changes characteristic of steatosis (Fig. 3), which were characterized by moderate alterations in all histopathological parameters analyzed (Fig. 4A–E). As a result, the NAFLD activity score (median ± interquartile range, 3 ± 2.5) indicated that HFD-fed $Nnt^{+/+}$ mice developed simple steatosis (Fig. 4F) (Kleiner et al.,

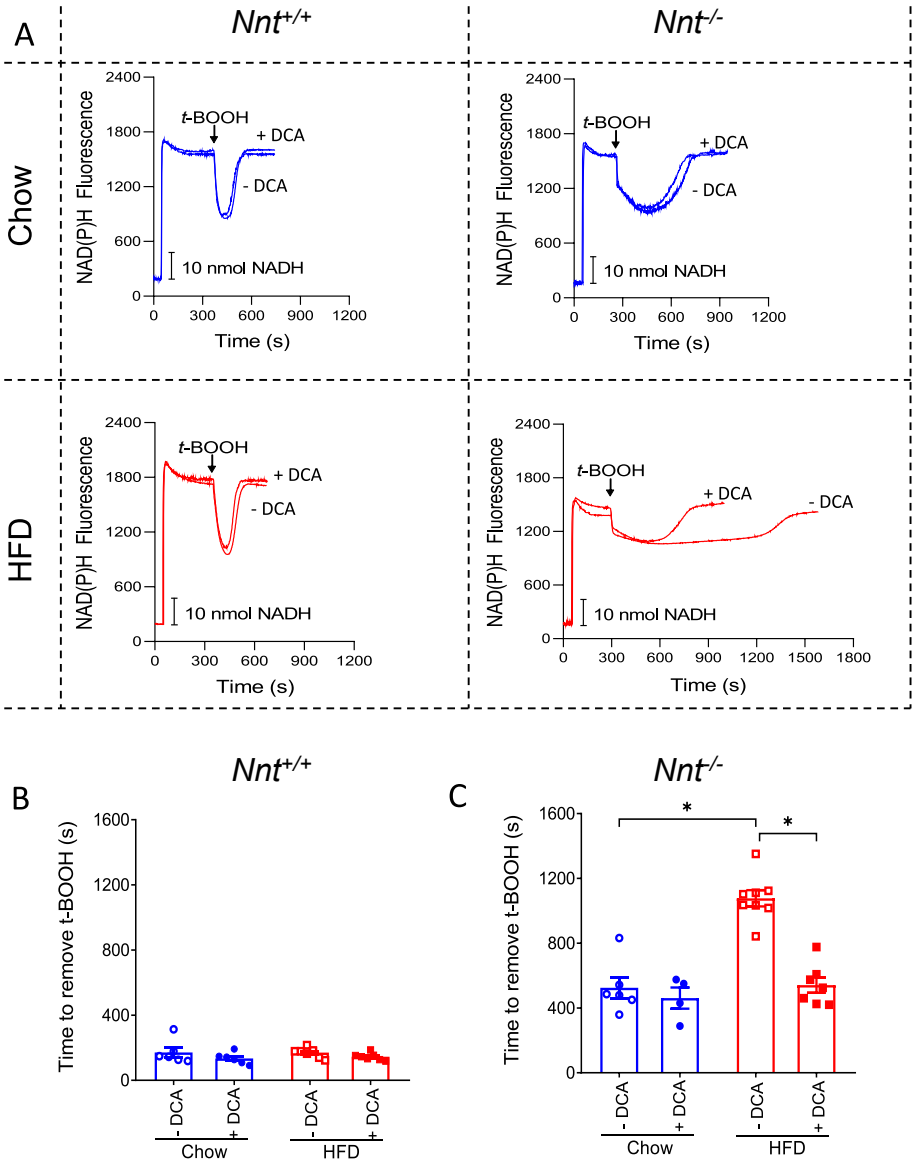

Fig. 1. – Dichloroacetate (DCA) restores the mitochondrial ability to metabolize organic peroxide, which is hampered in *Nnt*$^{-/-}$ mice under a high-fat diet (HFD). (A) Representative traces of endogenous fluorescence of NAD(P)H continuously monitored over time in isolated liver mitochondria (0.5 mg/mL) from *Nnt*$^{+/+}$ and *Nnt*$^{-/-}$ mice fed a chow diet or an HFD. Subgroups of mice were treated with DCA in their drinking water (+DCA) and compared to their respective controls (-DCA). *tert*-Butyl hydroperoxide (t-BOOH, 15 μM) was added to the reaction medium where indicated. The mitochondrial ability to metabolize peroxide was estimated by the time spent to recover the reduced state of NAD(P) following the addition of t-BOOH in *Nnt*$^{+/+}$ (B) and *Nnt*$^{-/-}$ (C) mouse mitochondria. N = 4–8. *$p < 0.0001$.

2005).

In line with our previous results (Navarro et al., 2017), in addition to the highest liver mass and triglyceride content (Tables 1 and 2, respectively), *Nnt*$^{-/-}$ mice on an HFD exhibited an aggravated form of NAFLD (Fig. 5), showing an increased frequency of microvesicular steatosis and higher grades of acinar and portal inflammation (Fig. 6A–E), thereby exhibiting scores indicative of NASH (median ± interquartile range, 7 ± 3.25) (Fig. 6F).

In *Nnt*$^{+/+}$ mice, DCA treatment did not significantly change liver mass and hepatic triglycerides content regardless of diet (Tables 1 and 2). However, in histopathological analysis, livers from DCA-treated chow-fed *Nnt*$^{+/+}$ mice showed increased hepatocyte ballooning, leading to a significant increase in the NAFLD activity score in this group (Figs. 3 and 4A). DCA treatment also increased hepatocyte ballooning in chow-fed *Nnt*$^{-/-}$ mice (Figs. 5 and 6A). Notably, DCA treatment in HFD-fed *Nnt*$^{-/-}$ mice resulted in lower liver mass and hepatic triglyceride content than vehicle-treated genotype-matched controls (Tables 1 and 2). Moreover, DCA treatment in HFD-fed *Nnt*$^{-/-}$ mice significantly prevented microvesicular steatosis and acinar/portal inflammation (Fig. 6B, D, E, and Supplementary Fig. S1), resulting in a significantly lower grade of NAFLD activity score (Fig. 6F).

3.5. DCA treatment decreased the level of pPDHE1α (S293) in HFD-fed *Nnt*$^{-/-}$ mice

Previous data demonstrated that the impaired mitochondrial peroxide removal in HFD-fed *Nnt*$^{-/-}$ mice are related to PDH inhibition due to phosphorylation of its subunits (Navarro et al., 2017). Here, levels of both total PDHE1α and pPDHE1α (S293) were assessed by western blotting in *Nnt*$^{+/+}$ and *Nnt*$^{-/-}$ mouse liver samples (Fig. 7). The expression levels of total PDHE1α were not changed by diet, treatment, or *Nnt* genotype (Fig. 7A and C). In contrast, the levels of pPDHE1α (S293) increased in HFD-fed *Nnt*$^{-/-}$ mice (Fig. 7C). Indeed, the ratio of pPDHE1α (S293) to total PDHE1α demonstrated PDH was relatively more phosphorylated in HFD-fed *Nnt*$^{-/-}$ mice than in other groups (Fig. 7B and D). Thus, DCA treatment restored the levels of pPDHE1α (S293) in *Nnt*$^{-/-}$ HFD-fed mice. The levels of pPDHE1α (S293) in chow-fed *Nnt*$^{-/-}$ or *Nnt*$^{+/+}$ mice on both diets remained unchanged by DCA treatment.

4. Discussion

HFD promotes NAFLD by a mechanism that involves liver mitochondrial dysfunctions and oxidative stress. These impairments are

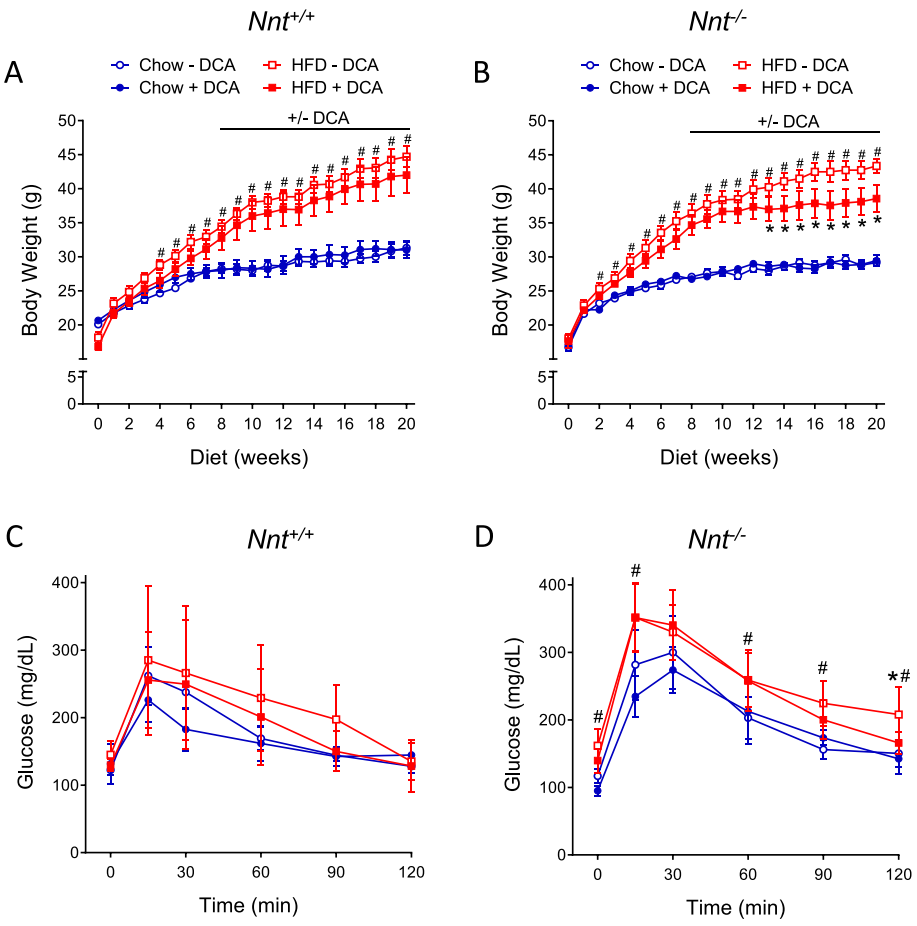

Fig. 2. - DCA treatment reduces body mass gain in $Nnt^{-/-}$ mice under an HFD and improves its late blood glucose levels in glucose tolerance test (GTT). Body mass changes in $Nnt^{+/+}$ (A) and $Nnt^{-/-}$ (B) mice over 20 weeks on chow or HFD. Mice subgroups were treated or not with DCA in the last 12 weeks as indicated. The glycemic response to the GTT in $Nnt^{+/+}$ (C) and $Nnt^{-/-}$ (D) mice were evaluated at the end of the treatments. N = 4–8. $^{*}p < 0.05$ *vs.* diet-matched mice at the respective time-points. $^{\#}p < 0.05$, "HFD - DCA" *vs.* "Chow - DCA" group at the respective time-points.

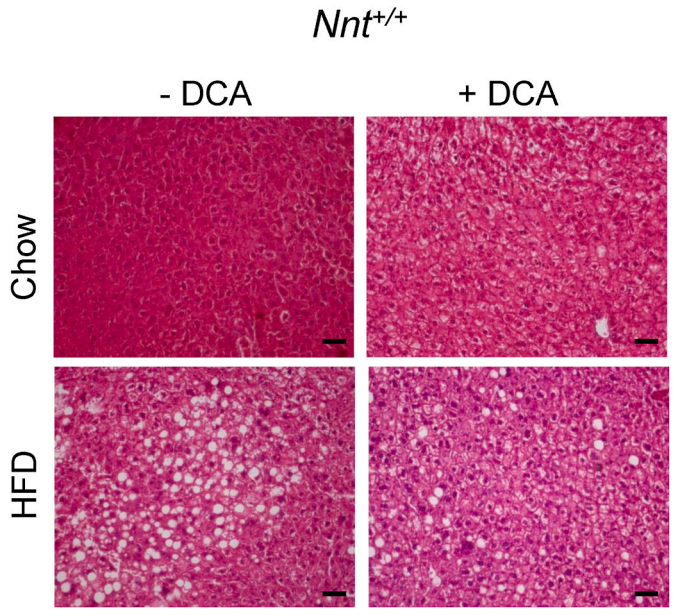

Fig. 3. - Representative liver sections stained with hematoxylin and eosin from chow and HFD-fed $Nnt^{+/+}$ mice. Mice subgroups were treated or not with DCA during the last 12 weeks as indicated. Scale bars: 50 μm. N = 6–8.

associated with lower ATP synthesis, increased inflammatory response, lower expression of AMP-activated protein kinase, and downregulation of the transcriptional coactivator peroxisome proliferator-activated receptor α (PPAR-α) (Echeverría et al., 2019; Ortiz et al., 2020; Videla and Valenzuela, 2021). Inhibition of mitochondrial pyruvate oxidation via PDH seems to be a replicable phenomenon following acute and chronic exposure to HFD (Alves et al., 2011; Go et al., 2016; Hwang et al., 2009; Navarro et al., 2017; Schummer et al., 2008; Tso et al., 2014; Wu et al., 2018). The downstream consequences of PDH inhibition are not fully understood; however, studies on mice have indicated that NAFLD and the abnormal metabolism of carbohydrate, fatty acid, and ketone bodies may be ameliorated when PDH activity is experimentally maintained or reestablished during conditions of dietary fat overload (Go et al., 2016; Hwang et al., 2009; Tso et al., 2014; Wu et al., 2018; Zhang et al., 2018). Significantly, most of what we know from these fundamental studies rely on experiments with mice models (e.g., C57BL/6J) that lack NNT activity due to a spontaneous *Nnt* mutation. We have previously demonstrated that another consequence of the HFD-induced PDH inhibition is a decreased rate of NADPH-dependent peroxide removal by isolated liver mitochondria from $Nnt^{-/-}$ mice when energy metabolism is sustained by pyruvate, which favors oxidative imbalance in this condition (Navarro et al., 2017).

Because oxidative imbalance is implicated in the pathogenesis of NAFLD and $Nnt^{-/-}$ mice develop aggravated forms of NAFLD when on an HFD (Navarro et al., 2017), we hypothesized that reactivation of PDH via the administration of DCA would result in both improved liver mitochondrial peroxide removal and attenuation of NAFLD in those mice. DCA is a pharmacological tool previously used to reactivate PDH in humans and experimental models (James et al., 2017). Here, the oral administration of DCA in the drinking water reactivated liver PDH in HFD-fed $Nnt^{-/-}$ mice, as evidenced by the reduction of pPDHE1α/PDHE1α ratio in these animals (Fig. 7). Significantly, DCA treatment restored pyruvate-supported peroxide removal by liver

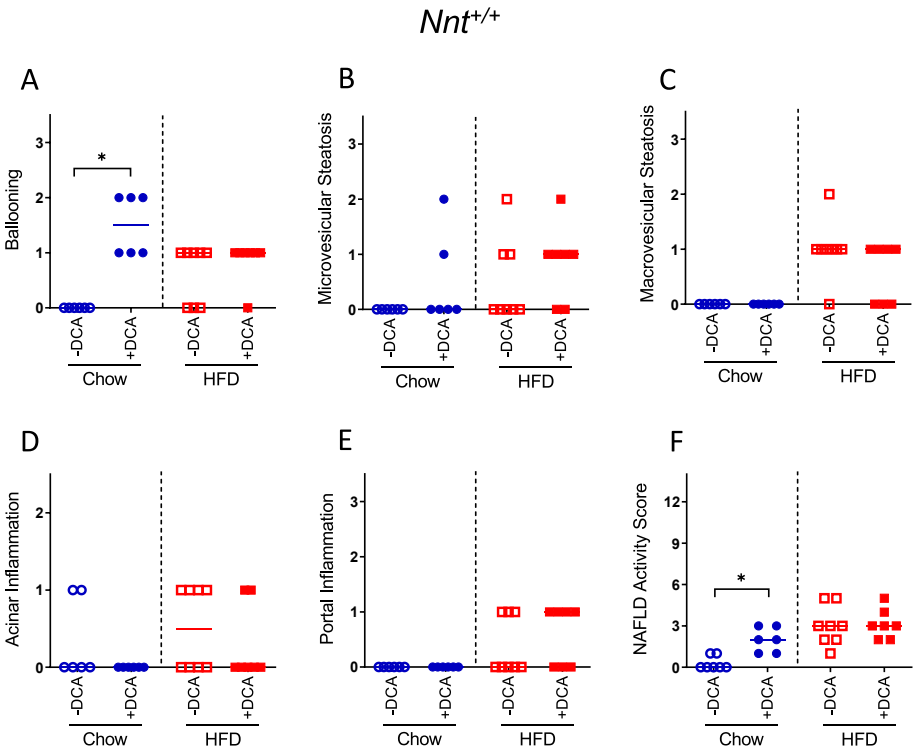

Fig. 4. - DCA treatment causes hepatocyte ballooning in *Nnt*$^{+/+}$ mice fed a chow diet. (A–E) Hepatic abnormalities scores in *Nnt*$^{+/+}$ mice fed a chow diet or HFD and treated (+DCA) or non-treated (-DCA) with DCA. Scores were graded according to Kleiner et al. (Kleiner et al., 2005). Individual scores from 0 to 3 were attributed to each hepatic alteration related to NAFLD. (F) NAFLD activity score was obtained from the sum of the scores presented in panels A–E. The higher is the NAFLD activity score, the worse the abnormality is. Only diet-matched mice groups were compared for statistical purposes, and actual *p*-values lower than 0.05 (*) are reported. N = 6–8.

Table 1
Liver mass (g) in *Nnt*$^{+/+}$ and *Nnt*$^{-/-}$ mice.

	Nnt$^{+/+}$		*Nnt*$^{-/-}$	
	-DCA	+DCA	-DCA	+DCA
Chow	1.5 ± 0.2	1.6 ± 0.3	1.7 ± 0.1	1.7 ± 0.1
HFD	2.0 ± 0.3[c]	1.9 ± 0.4	2.4 ± 1.0[b]	1.8 ± 0.1[a]

[a] $p < 0.01$ *vs* genotype and diet-matched mice.
[b] $p < 0.05$ *vs*. mice on chow diet of same genotype and treatment.
[c] $p < 0.001$ *vs*. mice on chow diet of same genotype and treatment.

Table 2
Hepatic triglycerides content (mg/g) in *Nnt*$^{+/+}$ and *Nnt*$^{-/-}$ mice.

	Nnt$^{+/+}$		*Nnt*$^{-/-}$	
	-DCA	+DCA	-DCA	+DCA
Chow	6.8 ± 5.7	6.9 ± 5.1	16.6 ± 5.6	17.3 ± 6.5
HFD	22.9 ± 18.1[b]	26.8 ± 10.9[b]	105.8 ± 24.8[c]	29.4 ± 18.9[a]

[a] $p < 0.001$ *vs*. genotype and diet-matched mice.
[b] $p < 0.05$ *vs*. mice on chow diet of same genotype and treatment.
[c] $p < 0.001$ *vs*. mice on chow diet of same genotype and treatment.

mitochondria to the genotype-control levels (Fig. 1). It is worth noting that in the absence of NADPH supply via NNT, pyruvate oxidative decarboxylation through PDH comprises a pathway providing isocitrate for IDH2, a concurrent source of mitochondrial NADPH.

Over the last decade, PDK2 or PDK4 knockout mice have been used as a model to demonstrate that metabolic diseases following HFD can be attenuated when PDH activity is preserved (Go et al., 2016; Hwang et al., 2009; Wu et al., 2018). While several novel PDK inhibitors have been tested, DCA is the prototypical pan-PDK inhibitor. DCA is a small hydrophilic compound that enters cells, and gains access to PDK within the mitochondrial matrix via membrane transporters such as monocarboxylate transporter 4 and sodium-coupled monocarboxylate transporter 1 (Babu et al., 2011; Jackson and Halestrap, 1996). By inhibiting PDK, DCA prevents the phosphorylation of PDHE1α and thus maintains

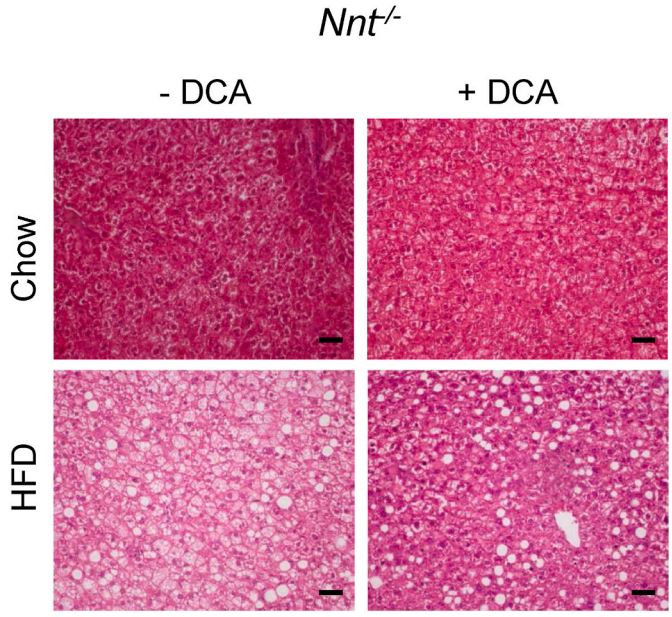

Fig. 5. - Representative liver sections stained with hematoxylin and eosin from chow and HFD-fed *Nnt*$^{-/-}$ mice. Mice subgroups were treated or not with DCA during the last 12 weeks as indicated. Scale bars: 50 μm. N = 4–8.

this enzyme in its active form (Rardin et al., 2009). In previous studies, DCA was promising for treating or alleviating impairments related to glucose oxidation, such as the dysregulated hepatocyte metabolism and mitochondrial dysfunction that occur in sepsis (Mainali et al., 2021), and it was proposed to treat human congenital lactic acidosis (James et al., 2017; Naveen Mangal et al., 2018). Antitumor effects of DCA have also been explored (Do Nascimento et al., 2021; Pajuelo-Reguera et al., 2015; Su and Lin, 2021).

Improvements in many metabolic indexes, including glucose

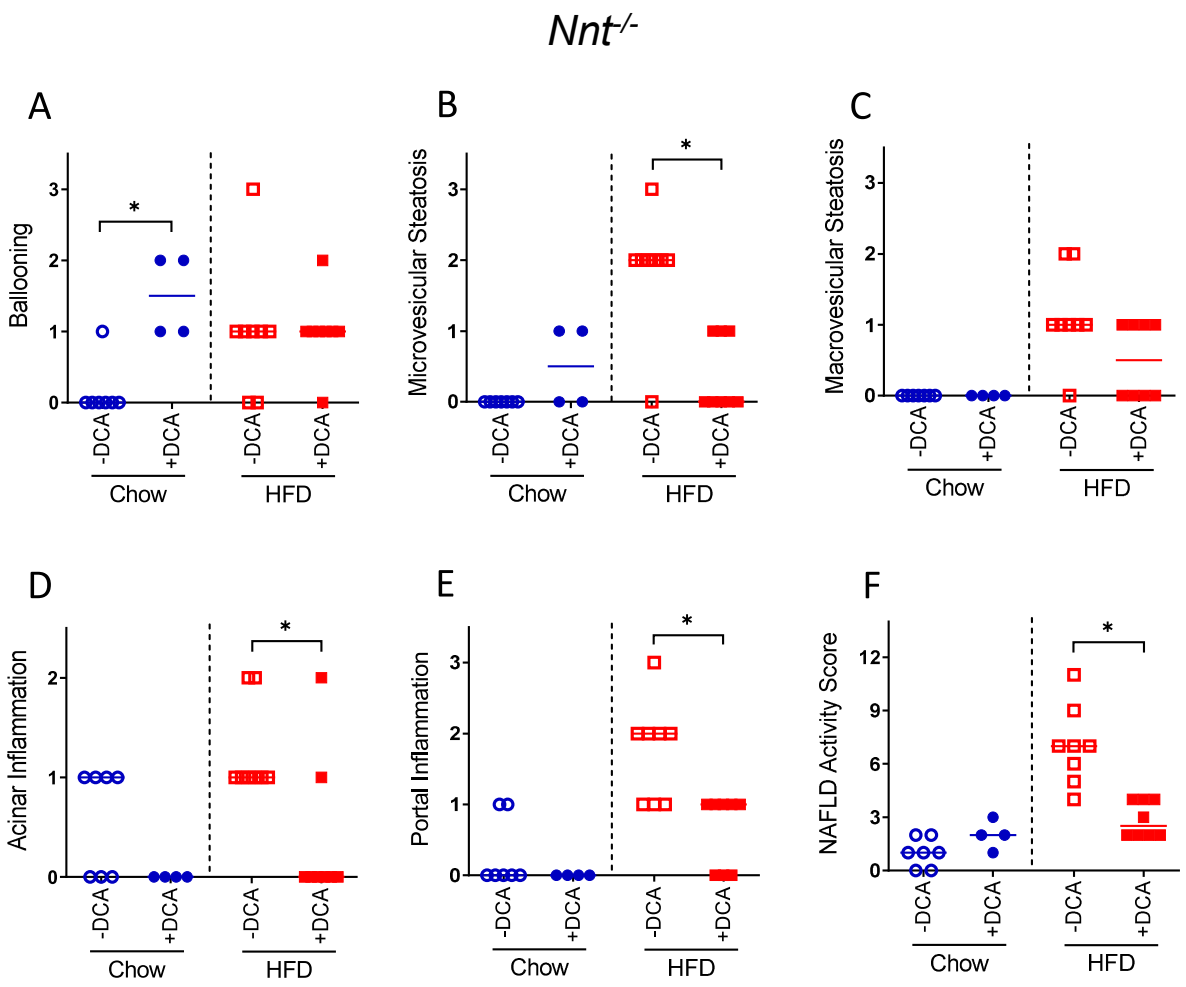

Fig. 6. DCA treatment prevents the progression of hepatic alterations related to non-alcoholic steatohepatitis (NASH) in *Nnt*$^{-/-}$ mice fed an HFD. (A–E) Hepatic abnormalities scores in *Nnt*$^{-/-}$ mice fed a chow diet or HFD and treated (+DCA) or non-treated (-DCA) with DCA. Scores were graded according to Kleiner et al. (Kleiner et al., 2005). Individual scores from 0 to 3 were attributed to each hepatic alteration related to NAFLD. (F) NAFLD activity score was obtained from the sum of the scores presented in panels A–E. The higher is the NAFLD activity score, the worse the abnormality is. Only diet-matched mice groups were compared for statistical purposes, and actual *p*-values lower than 0.05 (*) are reported. N = 4–8.

tolerance and hepatic lipid content, have been recently described following intraperitoneal administration of HFD-fed mice with DCA or its functional analog PS10 (Wu et al., 2018). However, that study did not evaluate the DCA effect on NAFLD or mitochondrial function. Moreover, the treatment with diisopropylamine dichloroacetate, a derivative of DCA, exerted beneficial effects on NAFLD patients (Lun-gen et al., 2005; Yan et al., 2013). In line with these findings, the oral DCA treatment improved several endpoints evaluated in HFD-fed *Nnt*$^{-/-}$ mice, such as body and liver mass, the content of hepatic triglycerides, glucose tolerance, and it prevented the aggravation of NAFLD (Figs. 2, 5 and 6, Tables 1 and 2).

Despite these beneficial effects observed in HFD-fed mice, DCA caused hepatocyte ballooning in the chow-fed groups (Figs. 3–6), which occurred in the absence of other hepatic abnormalities related to NAFLD and regardless of *Nnt* genotype. Ballooning injury is one of the histological hallmarks of NASH, and its formation may be mediated by glucose intolerance (Kakisaka et al., 2021). However, its occurrence in chow-fed mice in the absence of an increase in liver content of hepatic triglycerides draws attention to the possible toxic effects of DCA. It has been suggested that hepatocyte ballooning formation reflects alterations in the plasma membrane permeability and cytoskeletal derangements (Denk et al., 2019). Moreover, it can be associated with impaired cell death pathways (Suzuki et al., 2016). Ballooning has also been observed in the hepatic damage caused by xenobiotics, such as ethanol, CCl_4, and NaF (Avasarala et al., 2006; Bouaziz et al., 2006; Noyan et al., 2006; Okino et al., 1991). It is worth noting that although DCA was delivered at ~70% lower daily dose when compared to a previous study (Wu et al., 2018), route of administration (oral via drinking water vs. intraperitoneal injections) and longer duration of treatment (twelve vs. two weeks) may have favored the development of ballooning as DCA side effect.

Considering that proper dosing of DCA in chronic treatment is complicated because this compound inhibits its hepatic metabolism via cytosolic glutathione transferase (James and Stacpoole, 2016), DCA side effects such as hepatic toxicity could indeed arise. Hepatic toxicity of DCA is less studied than its peripheral nerve toxicity (James and Stacpoole, 2016; Stacpoole et al., 2019), but hepatomegaly has been reported in mice and dogs in response to the highest studied doses (Cicmanec et al., 1991; Hassoun et al., 2010). Despite the efficacy of DCA in reactivating pyruvate oxidative decarboxylation via PDH in various experimental settings (Stacpoole et al., 2019), further studies seem to be required for the understanding of how dose, route of administration, treatment length, age, and liver function may interact to

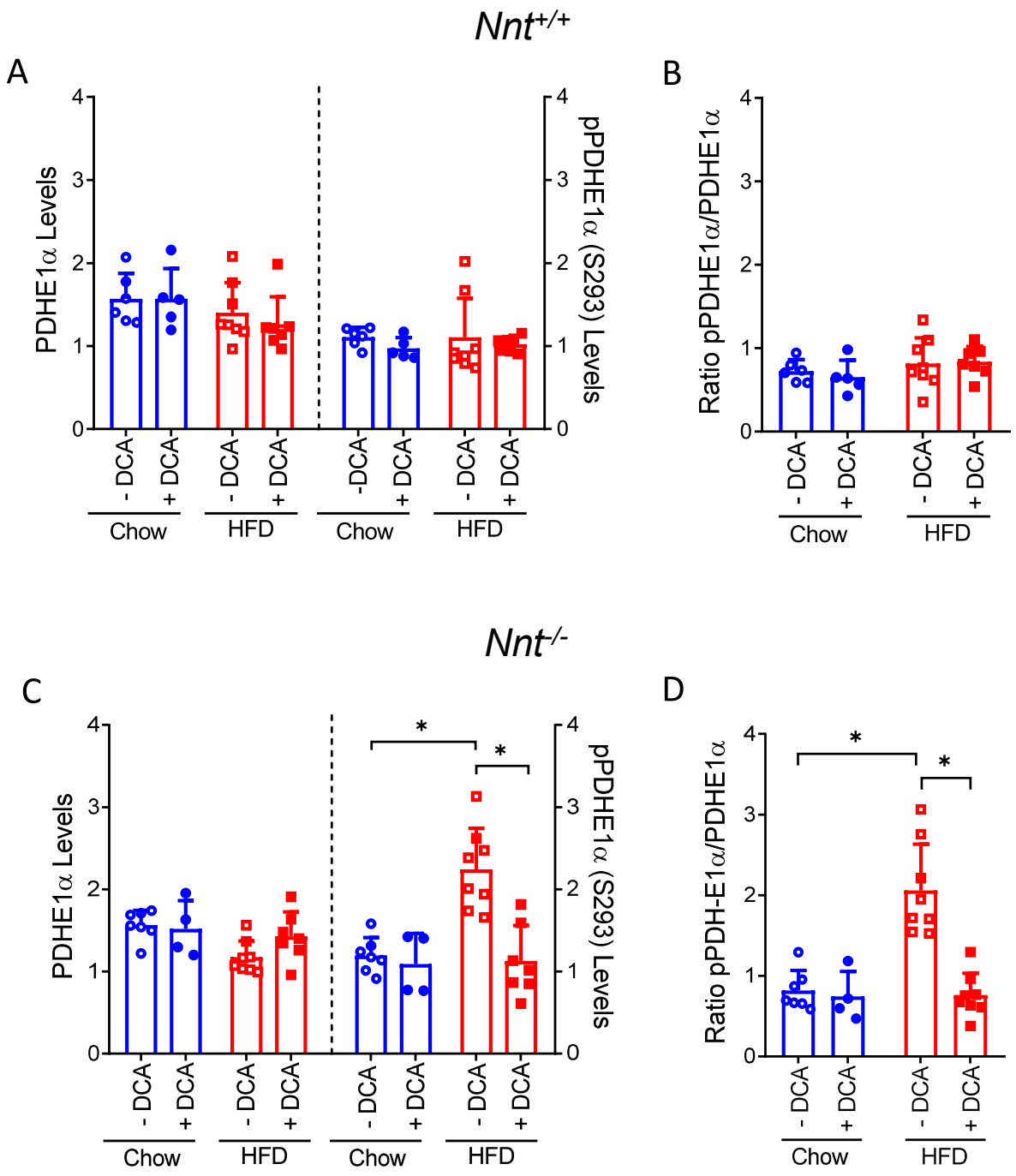

Fig. 7. DCA treatment reestablishes the level of PDHE1α phosphorylation at serine293 (S293) in liver mitochondria from $Nnt^{-/-}$ mice fed an HFD. Relative levels of total PDHE1α and phosphorylated PDHE1α ((pPDHE1α (S293)) by SDS-PAGE/Western blot in liver mitochondria samples (50 μg) from $Nnt^{+/+}$ (A) and $Nnt^{-/-}$ mice (C), calculated as the optical density of the bands normalized by the optical density of their respective loading controls (Supplementary Figs. S2 and S3). The ratios between the levels of pPDHE1α (S293) and PDHE1α in panels B and D represent the PDH phosphorylation state in $Nnt^{+/+}$ and $Nnt^{-/-}$ mice, respectively. N = 4–8. *$p < 0.01$.

generate side effects that outweigh the beneficial metabolic effects of DCA treatment on PDH activation.

We conclude that a moderate dose and long-term DCA treatment improved HFD-induced NAFLD in mice bearing the *Nnt* mutated alleles from the widely used C57BL/6J strain. Under these conditions, despite the efficacy of DCA in reactivating liver mitochondria pyruvate-supported peroxide removal and preventing NAFLD progression, the increased ballooning score in chow-fed mice treated with DCA draws attention to possible side effects of this drug that may be independent of its effects on PDH activity.

Declaration of competing interest

The authors declare that they have no known competing financial interests or personal relationships that could have appeared to influence the work reported in this paper.

CRediT authorship contribution statement

Claudia D.C. Navarro: Conceptualization, Methodology, Validation, Formal analysis, Investigation, Data curation, Visualization, Writing – original draft. **Annelise Francisco:** Investigation, Visualization, Writing – original draft. **Tiago R. Figueira:** Conceptualization, Writing – original draft. **Juliana A. Ronchi:** Resources. **Helena C.F. Oliveira:** Methodology, Writing – review & editing. **Anibal E. Vercesi:** Conceptualization, Funding acquisition, Supervision, Writing – review & editing. **Roger F. Castilho:** Conceptualization, Formal analysis, Supervision, Writing – review & editing, Project administration, Funding acquisition.

Acknowledgments

We are thankful to Edilene S. Siqueira-Santos for technical assistance. This work was supported by the São Paulo Research Foundation (FAPESP, grant numbers 17/17728-8, 19/20855-7 and 20/05202-4) and the Brazilian National Council for Scientific and Technological Development (CNPq).

Appendix A. Supplementary data

Supplementary data to this article can be found online at https://doi.org/10.1016/j.ejphar.2022.174750.

References

Agledal, L., Niere, M., Ziegler, M., 2010. The phosphate makes a difference: cellular functions of NADP. Redox Rep. 15, 2–10. https://doi.org/10.1179/174329210X12650506623122.

Alves, T.C., Befroy, D.E., Kibbey, R.G., Kahn, M., Codella, R., Carvalho, R.A., Falk Petersen, K., Shulman, G.I., 2011. Regulation of hepatic fat and glucose oxidation in rats with lipid-induced hepatic insulin resistance. Hepatology 53, 1175–1181. https://doi.org/10.1002/hep.24170.

Andreassen, O.A., Ferrante, R.J., Huang, H.-M., Dedeoglu, A., Park, L., Kimberly, L., Ferrante, B., Jennifer Kwon, B., Borchelt, D.R., Ross, C.A., Gibson, G.E., Flint Beal, M., Dichloroacetate, M., 2001. Dichloroacetate exerts therapeutic effects in transgenic mouse models of huntington's disease. Ann. Neurol. 50, 112–116. https://doi.org/10.1002/ana.1084.

Avasarala, S., Yang, L., Sun, Y., Leung, A.W.C., Chan, W.Y., Cheung, W.T., Lee, S.S.T., 2006. A temporal study on the histopathological, biochemical and molecular responses of CCl4-induced hepatotoxicity in Cyp2e1-null mice. Toxicology 228, 310–322. https://doi.org/10.1016/j.tox.2006.09.019.

Babu, E., Ramachandran, S., CoothanKandaswamy, V., Elangovan, S., Prasad, P.D., Ganapathy, V., Thangaraju, Muthusamy, 2011. By inhibiting PDK, dichloroacetate prevents the phosphorylation of E1α and thus maintains PDC in active form. Oncogene 30, 4026–4037. https://doi.org/10.1038/onc.2011.113. Role.

Bian, L., Josefsson, E., Jonsson, I.M., Verdrengh, M., Ohlsson, C., Bokarewa, M., Tarkowski, A., Magnusson, M., 2009. Dichloroacetate alleviates development of collagen II-induced arthritis in female DBA/1 mice. Arthritis Res. Ther. 11, 1–10. https://doi.org/10.1186/ar2799.

Bouaziz, H., Ketata, S., Jammoussi, K., Boudawara, T., Ayedi, F., Ellouze, F., Zeghal, N., 2006. Effects of sodium fluoride on hepatic toxicity in adult mice and their suckling pups. Pestic. Biochem. Physiol. 86, 124–130. https://doi.org/10.1016/j.pestbp.2006.02.004.

Buettner, R., Scholmerich, J., Bollheimer, L.C., 2007. High-fat diets: modeling the metabolic disorders of human obesity in rodents. Obesity 15, 798–808. https://doi.org/10.1038/oby.2007.608.

Chalasani, N., Younossi, Z., Lavine, J.E., Diehl, A.M., Brunt, E.M., Cusi, K., Charlton, M., Sanyal, A.J., 2012. The diagnosis and management of non-alcoholic fatty liver disease: practice guideline by the American association for the study of liver diseases, American college of gastroenterology, and the American gastroenterological association. Hepatology 55. https://doi.org/10.1002/hep.25762, 2005–2023.

Cicmanec, J.L., Condie, L.W., Olson, G.R., Wang, S.-R., 1991. 90-Day toxicity study of dichloroacetate in dogs. Toxicol. Sci. 17, 376–389. https://doi.org/10.1093/toxsci/17.2.376.

Denk, H., Abuja, P.M., Zatloukal, K., 2019. Animal models of NAFLD from the pathologist's point of view. Biochim. Biophys. Acta (BBA) - Mol. Basis Dis. 1865, 929–942. https://doi.org/10.1016/j.bbadis.2018.04.024.

Do Nascimento, R.S., Nagamine, M.K., De Toledo, G.F., Chaible, L.M., Tedardi, M.V., Del-Grande, M.P., Da Fonseca, I.I.M., Dagli, M.L.Z., 2021. Sodium dichloroacetate attenuates the growth of B16-F10 melanoma in vitro and in vivo: an opportunity for drug repurposing. Anti Cancer Drugs 111–116. https://doi.org/10.1097/CAD.0000000000001013.

Echeverría, F., Valenzuela, R., Bustamante, A., Álvarez, D., Ortiz, M., Espinosa, A., Illesca, P., Gonzalez-Manañ, D., Videla, L.A., 2019. High-fat diet induces mouse liver steatosis with a concomitant decline in energy metabolism: attenuation by eicosapentaenoic acid (EPA) or hydroxytyrosol (HT) supplementation and the additive effects upon EPA and HT co-administration. Food Funct. 10, 6170–6183. https://doi.org/10.1039/c9fo01373c.

Fisher-Wellman, K.H., Ryan, T.E., Smith, C.D., Gilliam, L.A.A., Lin, C.-T., Reese, L.R., Torres, M.J., Neufer, P.D., 2016. A direct comparison of metabolic responses to high-fat diet in C57BL/6J and C57BL/6NJ mice. Diabetes 65, 3249–3261. https://doi.org/10.2337/db16-0291.

Francisco, A., Ronchi, J.A., Navarro, C.D.C., Figueira, T.R., Castilho, R.F., 2018. Nicotinamide nucleotide transhydrogenase is required for brain mitochondrial redox balance under hampered energy substrate metabolism and high-fat diet. J. Neurochem. 147, 663–677. https://doi.org/10.1111/jnc.14602.

Francisco, A., Figueira, T.R., Castilho, R.F., 2021. Mitochondrial NAD(P) + transhydrogenase: from molecular Features to physiology and disease, 00 Antioxidants Redox Signal. 1–21. https://doi.org/10.1089/ars.2021.0111.

Go, Y., Jeong, J.Y., Jeoung, N.H., Jeon, J.H., Park, B.Y., Kang, H.J., Ha, C.M., Choi, Y.K., Lee, S.J., Ham, H.J., Kim, B.G., Park, K.G., Park, S.Y., Lee, C.H., Choi, C.S., Park, T.S., Lee, W.N., Harris, R.A., Lee, I.K., 2016. Inhibition of pyruvate dehydrogenase kinase 2 protects against hepatic steatosis through modulation of TCA cycle anaplerosis and ketogenesis. Diabetes 65, 2876–2887. https://doi.org/10.2337/db16-022.

Hassoun, E.A., Cearfoss, J., Spildener, J., 2010. Dichloroacetate-and trichloroacetate-induced oxidative stress in the hepatic tissues of mice after long term exposure. J. Appl. Toxicol. 30, 450–456. https://doi.org/10.1002/jat.1516.

Hwang, B., Jeoung, N.H., Harris, R.A., 2009. Pyruvate dehydrogenase kinase isoenzyme 4 (PDHK4) deficiency attenuates the long-term negative effects of a high-saturated fat diet. Biochem. J. 423, 243–252. https://doi.org/10.1042/BJ20090390.

Jackson, V.N., Halestrap, A.P., 1996. The kinetics, substrate, and inhibitor specificity of the monocarboxylate (lactate) transporter of rat liver cells determined using the fluorescent intracellular pH indicator, 2′,7′-bis(carboxyethyl)-5(6)-carboxyfluorescein. J. Biol. Chem. 271, 861–868. https://doi.org/10.1074/jbc.271.2.861.

James, M.O., Stacpoole, P.W., 2016. Pharmacogenetic considerations with dichloroacetate dosing. Pharmacogenomics 17, 743. https://doi.org/10.2217/PGS-2015-0012.

James, M.O., Jahn, S.C., Zhong, G., Smeltz, M.G., Hu, Z., Stacpoole, P.W., Hu, Zhiwei, Stacpoole, P.W., 2017. Therapeutic applications of dichloroacetate and the role of glutathione transferase zeta-1. Pharmacol. Ther. 170, 166–180. https://doi.org/10.1016/j.pharmthera.2016.10.018.Therapeutic.

Kakisaka, K., Sasaki, A., Umemura, A., Nikai, H., Suzuki, Y., Nishiya, M., Sugai, T., Nitta, H., Takikawa, Y., 2021. High frequency and long persistency of ballooning hepatocyte were associated with glucose intolerance in patients with severe obesity. Sci. Rep. 11, 1–9. https://doi.org/10.1038/s41598-021-94937-4.

Kleiner, D.E., Brunt, E.M., Van Natta, M., Behling, C., Contos, M.J., Cummings, O.W., Ferrell, L.D., Liu, Y.C., Torbenson, M.S., Unalp-Arida, A., Yeh, M., McCullough, A.J., Sanyal, A.J., 2005. Design and validation of a histological scoring system for nonalcoholic fatty liver disease. Hepatology 41, 1313–1321. https://doi.org/10.1002/hep.20701.

Lingohr, M.K., Thrall, B.D., Bull, R.J., 2001. Effects of dichloroacetate (DCA) on serum insulin levels and insulin-controlled signaling proteins in livers of male B6C3F1 mice. Toxicol. Sci. 59, 178–184. https://doi.org/10.1093/toxsci/59.1.178.

Lun-gen, L., Min-de, Z., Yi-min, M., Cheng-ei, C., Qing-chun, F., Ji-yao, W., Wei-fen, X., Jian-gao, F., Dong-feng, C., Bing-yuan, W., 2005. Diisopropylamine dichloroacetate in the treatment of nonalcoholic fatty liver disease: a multicenter random double-blind controlled trial. Chin. J. Hepatol. 13, 92–95.

Mailloux, R.J., 2018. Mitochondrial antioxidants and the maintenance of cellular hydrogen peroxide levels. Oxid. Med. Cell. Longev. 7857251. https://doi.org/10.1155/2018/7857251, 2018.

Mainali, R., Zabalawi, M., Long, D., Buechler, N., Quillen, E., Key, C.C., Zhu, X., Parks, J. S., Furdui, C., Stacpoole, P.W., Martinez, J., McCall, C.E., Quinn, M.A., 2021. Dichloroacetate reverses sepsis-induced hepatic metabolic dysfunction. Elife 10, 1–20. https://doi.org/10.7554/eLife.64611.

Mangal, Naveen, James, M.O., Stacpoole, P.W., Schmidt, S., 2018. Model informed dose optimization of dichloroacetate for the treatment of congenital lactic acidosis in children. J. Clin. Pharmacol. 58, 212–220. https://doi.org/10.1002/jcph.1009.Model.

Mantena, S.K., King, A.L., Andringa, K.K., Eccleston, H.B., Bailey, S.M., 2008. Mitochondrial dysfunction and oxidative stress in the pathogenesis of alcohol and obesity induced fatty liver diseases. Free Radic. Biol. Med. 44, 1259–1272. https://doi.org/10.1016/j.freeradbiomed.2007.12.029.

Mapes, J.P., Harris, R.A., 1975. Regulatory function of pyruvate dehydrogenase and the mitochondrion in lipogenesis. Lipids 10, 757–764. https://doi.org/10.1007/bf02532317.

Muriel, P., López-sánchez, P., Ramos-tovar, E., 2021. Fructose and the liver. Int. J. Mol. Sci. 22 https://doi.org/10.3390/ijms22136969.

Navarro, C.D.C., Figueira, T.R., Francisco, A., Dal'Bó, G.A., Ronchi, J.A., Rovani, J.C., Escanhoela, C.A.F., Oliveira, H.C.F., Castilho, R.F., Vercesi, A.E., 2017. Redox

imbalance due to the loss of mitochondrial NAD(P)-transhydrogenase markedly aggravates high fat diet-induced fatty liver disease in mice. Free Radic. Biol. Med. 113, 190–202. https://doi.org/10.1016/j.freeradbiomed.2017.09.026.

Noyan, T., Kömüroğlu, U., Bayram, I., Şekeroğlu, M.R., 2006. Comparison of the effects of melatonin and pentoxifylline on carbon tetrachloride-induced liver toxicity in mice. Cell Biol. Toxicol. 22, 381–391. https://doi.org/10.1007/s10565-006-0019-y.

Okino, T., Nakajima, T., Nakano, M., 1991. Morphological and biochemical analyses of trichloroethylene hepatotoxicity: differences in ethanol- and phenobarbital-pretreated rats. Toxicol. Appl. Pharmacol. 108, 379–389. https://doi.org/10.1016/0041-008X(91)90084-R.

Ortiz, M., Soto-Alarcón, S.A., Orellana, P., Espinosa, A., Campos, C., López-Arana, S., Rincón, M.A., Illesca, P., Valenzuela, R., Videla, L.A., 2020. Suppression of high-fat diet-induced obesity-associated liver mitochondrial dysfunction by docosahexaenoic acid and hydroxytyrosol co-administration. Dig. Liver Dis. 52, 895–904. https://doi.org/10.1016/j.dld.2020.04.019.

Pajuelo-Reguera, D., Alán, L., Olejár, T., Ježek, P., 2015. Dichloroacetate stimulates changes in the mitochondrial network morphology via partial mitophagy in human SH-SY5Y neuroblastoma cells. Int. J. Oncol. 46, 2409–2418. https://doi.org/10.3892/ijo.2015.2953.

Rardin, M.J., Wiley, S.E., Naviaux, R.K., Murphy, A.N., Dixon, J.E., 2009. Monitoring phosphorylation of the pyruvate dehydrogenase complex. Anal. Biochem. 389, 157–164. https://doi.org/10.1016/j.ab.2009.03.040.

Ronchi, J.A., Figueira, T.R., Ravagnani, F.G., Oliveira, H.C.F., Vercesi, A.E., Castilho, R. F., 2013. A spontaneous mutation in the nicotinamide nucleotide transhydrogenase gene of C57BL/6J mice results in mitochondrial redox abnormalities. Free Radic. Biol. Med. 63, 446–456. https://doi.org/10.1016/j.freeradbiomed.2013.05.049.

Ronchi, J.A., Francisco, A., Passos, L.A.C., Figueira, T.R., Castilho, R.F., 2016. The contribution of nicotinamide nucleotide transhydrogenase to peroxide detoxification is dependent on the respiratory state and counterbalanced by other sources of NADPH in liver mitochondria. J. Biol. Chem. 291, 20173–20187. https://doi.org/10.1074/jbc.M116.730473.

Saed, C.T., Tabatabaei Dakhili, S.A., Ussher, J.R., 2021. Pyruvate dehydrogenase as a therapeutic target for nonalcoholic fatty liver disease. ACS Pharmacol. Transl. Sci. 4, 582–588. https://doi.org/10.1021/acsptsci.0c00208.

Schummer, C.M., Werner, U., Tennagels, N., Schmoll, D., Haschke, G., Juretschke, H.P., Patel, M.S., Gerl, M., Kramer, W., Herling, A.W., 2008. Dysregulated pyruvate dehydrogenase complex in Zucker diabetic fatty rats. Am. J. Physiol. Endocrinol. Metab. 294, E88–E96. https://doi.org/10.1152/ajpendo.00178.2007.

Spahis, S., Delvin, E., Borys, J.M., Levy, E., 2016. Oxidative stress as a critical factor in nonalcoholic fatty liver disease pathogenesis. Antioxidants Redox Signal. 26, 519–541. https://doi.org/10.1089/ars.2016.6776.

Stacpoole, P.W., Martyniuk, C.J., James, M.O., 2019. Dichloroacetate-induced peripheral neuropathy. Int. Rev. Neurobiol. 145, 211–238. https://doi.org/10.1016/BS.IRN.2019.05.003.

Su, D., Lin, Z., 2021. Dichloroacetate attenuates the stemness of hepatocellular carcinoma cells via promoting nucleus-cytoplasm translocation of YAP. Environ. Toxicol. 36, 975–983. https://doi.org/10.1002/tox.23098.

Suzuki, A., Kakisaka, K., Suzuki, Y., Wang, T., Takikawa, Y., 2016. C-Jun N-terminal kinase-mediated Rubicon expression enhances hepatocyte lipoapoptosis and promotes hepatocyte ballooning. World J. Gastroenterol. 22, 6509–6516. https://doi.org/10.3748/wjg.v22.i28.6509.

Tso, S.C., Qi, X., Gui, W.J., Wu, C.Y., Chuang, J.L., Wernstedt-Asterholm, I., Morlock, L. K., Owens, K.R., Scherer, P.E., Williams, N.S., Tambar, U.K., Wynn, R.M., Chuang, D. T., 2014. Structure-guided development of specific pyruvate dehydrogenase kinase inhibitors targeting the ATP-binding pocket. J. Biol. Chem. 289, 4432–4443. https://doi.org/10.1074/jbc.M113.533885.

Vercesi, A.E., Castilho, R.F., Kowaltowski, A.J., de Oliveira, H.C.F., de Souza-Pinto, N.C., Figueira, T.R., Busanello, E.N.B., 2018. Mitochondrial calcium transport and the redox nature of the calcium-induced membrane permeability transition. Free Radic. Biol. Med. 129, 1–24. https://doi.org/10.1016/j.freeradbiomed.2018.08.034.

Videla, L.A., Valenzuela, R., 2021. Perspectives in liver redox imbalance: toxicological and pharmacological aspects underlying iron overloading, nonalcoholic fatty liver disease, and thyroid hormone action. Biofactors. https://doi.org/10.1002/biof.1797.

Wu, C.-Y., Tso, S.-C., Chuang, J.L., Gui, W.-J., Lou, M., Sharma, G., Khemtong, C., Qi, X., Wynn, R.M., Chuang, D.T., 2018. Targeting hepatic pyruvate dehydrogenase kinases restores insulin signaling and mitigates ChREBP-mediated lipogenesis in diet-induced obese mice. Mol. Metabol. 12, 12–24. https://doi.org/10.1016/J.MOLMET.2018.03.014.

Yan, S., Yi-xuan, Z., Ya-rong, L., Da-wen, X., Bao-rong, C., 2013. Curative effects of compound diisopropylamine dichloroacetate injection on fatty liver disease induced by tamoxifen. J. Jilin Univ. (Sci. Ed.) 39, 152–155. https://doi.org/10.7694/jldxyxb20130134.

Zhang, M., Zhao, Y., Li, Z., Wang, C., 2018. Pyruvate dehydrogenase kinase 4 mediates lipogenesis and contributes to the pathogenesis of nonalcoholic steatohepatitis. Biochem. Biophys. Res. Commun. 495, 582–586. https://doi.org/10.1016/j.bbrc.2017.11.054.